Atomic details of step flow growth on Si(001)

J. van Wingerden, A. van Dam, M. J. Haye, P. M. L. O. Scholte, and F. Tuinstra
Department of Applied Physics, Delft University of Technology, Lorentzweg 1, 2628 CJ Delft, The Netherlands
(Received 31 July 1996)

Growth at step edges by the addition of single adatoms has been studied using scanning tunneling microscopy (STM). It is shown that the use of empty-state instead of filled-state STM images enables the assessment of the binding sites of single adatoms at step edges. We describe all different step edge configurations obtained by subsequently sticking adatoms to these step edges. Adatom diffusion along step edges as well as the dimerization of adatoms at a step edge are also demonstrated. Finally, the creation of single dimer vacancies at step edges is discussed. [S0163-1829(97)01412-4]

Step edges form the crucial growth template during epitaxial growth. In the step-flow growth mode the mobility is high enough for all growth units to reach the step edges and stick there before a new growth center is nucleated. These step edges either originate from a macroscopic misalignment of the surface relative to the crystallographic plane or from dislocations terminating at the surface. In case the mobility of the growth units is insufficient to reach existing steps, islands nucleate on the terraces. The majority of the growth units then sticks to the newly created step edges of the islands. Thus, growth mechanisms at step edges play a decisive role in the step flow as well as the island growth mode.

Steps on the Si(001) surface have been investigated extensively, both because of the technological importance of this surface and because of its suitability as a model system for epitaxial growth studies. If the Si(001) surface is miscut towards the [110] direction, two types of monatomic steps are created on the surface. They differ in their orientation relative to the dimer rows to the (2×1) reconstructed terrace. For the so-called S_B type the dimer rows on the upper terrace are perpendicular to the step edge while they are parallel to the step edge for the S_A type.[1] If the average step edge direction is not along the [110] direction, the step edge consists of segments of both types.

The sticking probability for growth units is much larger at S_B than at the S_A type step edges.[2] Therefore, growth mainly occurs at S_B step edges. Two different types of S_B step edges exist, the so-called rebonded and nonrebonded S_B step edge.[1,3] They are alternatingly obtained by the subsequent addition of single ad dimers. Because the rebonded S_B step edge has a significantly lower energy it dominates the structure of the S_B steps. Thermally induced step edge fluctuations[4–8] have been studied with scanning tunneling microscopy (STM) at slightly elevated temperatures. Due to the predominant formation of the rebonded S_B step edge, only the attachment or removal of units of two dimers, i.e., four atoms, was observed. Whether adatoms or ad dimers are the smallest entities involved in the dynamic processes at the step edge is still unknown. Although single adatoms on Si(001) terraces and in clusters have been observed with STM before,[9,10] the interactions of single adatoms with step edges have only been studied theoretically.[11–13]

In the present work we describe experiments which reveal the growth process of S_B step edges on the level of single atoms. Growth at step edges with single adatoms is obtained by room temperature deposition of a submonolayer of silicon on Si(001). The S_B step edges on the as-grown surface have been studied with STM. As we will show the use of empty state instead of filled state STM images is a major tool for the determination of the binding sites for single adatoms. Based on these images we will first discuss the stable configurations formed upon the subsequent addition of single adatoms at step edges. Then, the dynamic processes at the step edge are discussed. The diffusion of adatoms along the step edge and the formation of a dimer at the step edge are illustrated with STM images. Furthermore, it is discussed how a particular step edge configuration can serve as a favorable site for the creation of single dimer vacancies.

The experiments have been performed in a UHV system with a base pressure of 5×10^{-11} Torr. A 10 s flash at 1250 °C is used for preparing the Si(001) substrates. Room temperature deposition of submonolayers of silicon on the substrates is performed with a commercial miniature electron-beam evaporator. During room temperature deposition most of the deposited material nucleates islands on the terraces.[14] A small amount of the deposited material is not incorporated in the islands on the terrace, but sticks to the monatomic height steps. The resulting step edge configurations are studied with a Beetle-type STM.[15] All STM images are measured in the constant current mode. Dynamic processes are studied by capturing images of the same surface area at 10 s time intervals. The observed changes may be induced by the electric field but they are most likely to be the relevant ones at slightly elevated temperatures.[16]

STM images of the configurations that have been encountered are shown in Fig. 1. Schematic drawings of the configurations and their abundances are shown in Fig. 2. The abundances are determined by counting the number of occurrences of different configurations observed in three experiments with room temperature deposited coverages ranging from 0.003 ML to 0.012 ML. The abundances are based on the configurations of over 2000 dimer rows ending at a step edge. Although some defects have been observed close to the step edges, no correlation between defects and certain atomic configurations was observed. The majority of the dimer rows ends with a dimer in the trough of the lower terrace [see configuration 0 in Figs. 1(a) and 1(b); note the pronounced appearance of the lower terrace dangling bonds in the empty-

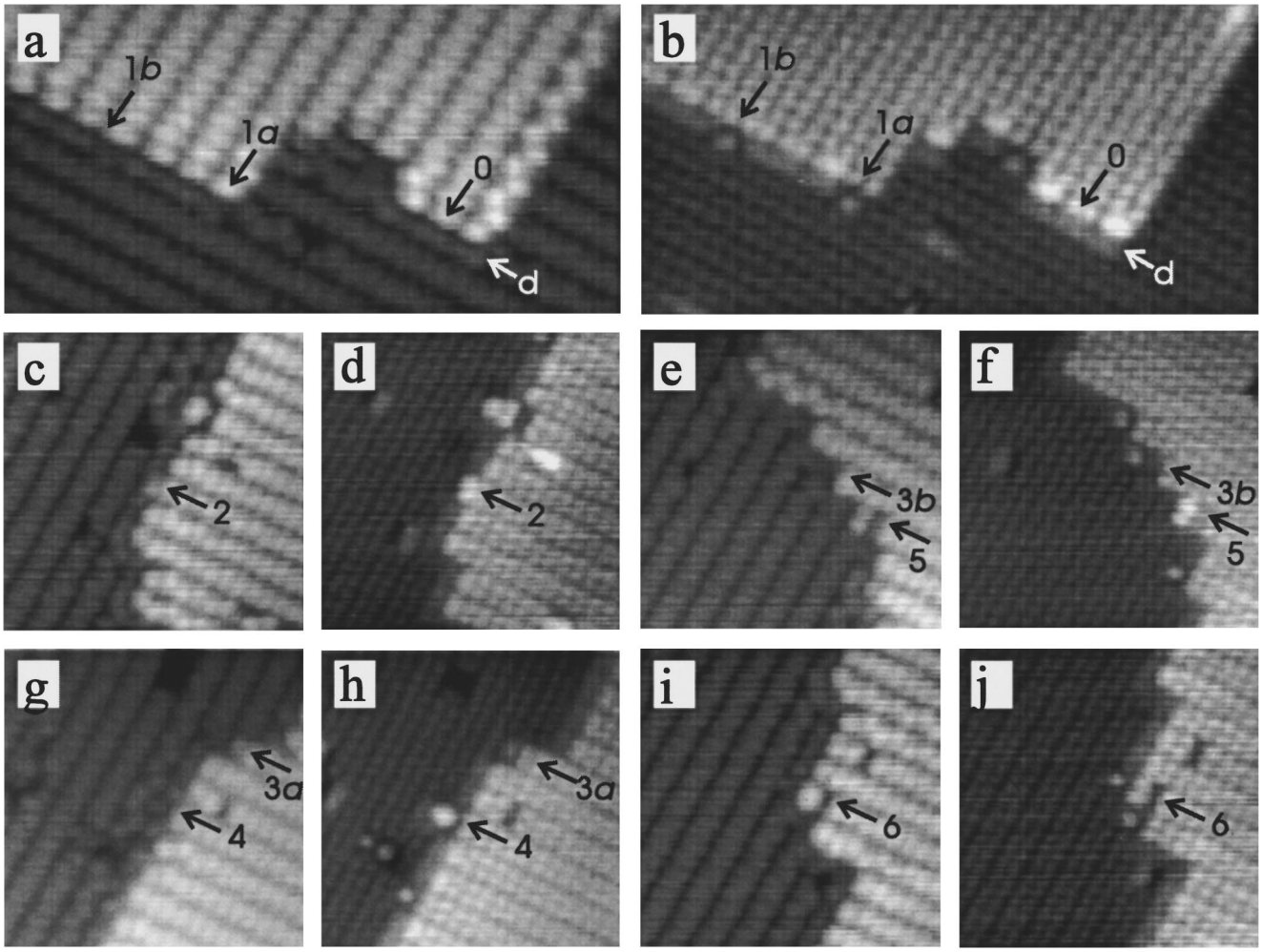

FIG. 1. Filled (a, c, e, g, i) and empty-state (b, d, f, h, j) STM images of step edges showing nine different configurations of dimer rows ending at S_B step edges (0, 1a, 1b, 2, 3a, 3b, 4, 5, and 6). The row of dangling bonds at the step edge in configuration 0 is indicated with d (a,b). Tunneling conditions: 1.5 nA (a,b), 1.1 nA (c–j); 1.3 V (a, c, e, g, i), −1.3 V (b, f, h, j) −1.0 V (d).

state image (b)]. This so-called rebonded S_B step edge is the only configuration observed on the surfaces before growth. Thus we consider configuration 0 as the starting point for the growth process. The configurations 1a and 1b represent the two inequivalent stable binding sites for single adatoms. It should be noted that the single adatoms are clearly visible in the empty-state image while they are nearly invisible in the filled-state image. This is a general observation which is also valid for the visibility of single adatoms in other configurations.[14,18] Positioning the adatom at the center of the dimer row (configuration 1a) gas a thirty times higher population than the site of configuration 1b. The dimer row of the upper terrace can be extended with a dimer by adding another adatom. Now, the dimer row ends with a dimer on top of the row of the lower terrace. This configuration [2 in Figs. 1(c) and 1(d)] is usually indicated as a nonrebonded S_B step edge. It has only been observed at the end of 0.5% of the dimer rows. While configuration 2 is already very rare, we have even fewer images of the next step, where another adatom is added. Configuration 3a [see Figs. 1(g) and 1(h)] shows the binding of an adatom to the same dimer row of the lower terrace on top of which the step edge ends. This configuration has been observed only once. Furthermore, we observed a configuration [3b in Figs. 1(g) and 1(h)] where the adatom is attached to the next row of the lower terrace. This configuration has been observed five times and in all of these cases the binding of the adatom seems to be stabilized by a neighboring S_A step edge. if step flow growth proceeds by the addition of single adatoms, the step edge starts from configuration 0 and subsequently assumes the above mentioned configurations 1a or 1b, 2, 3a or 3b, and finally configuration 0 again.

Competitive processes may ''block'' the growth process, yielding different structures. For example, we observed that at the end of 4% of the dimer rows a nonepitaxial dimer is

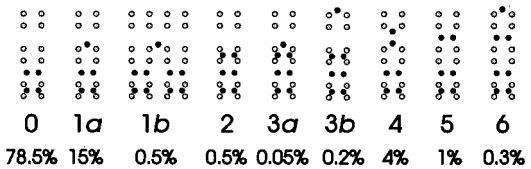

FIG. 2. Schematic representation of the different atomic configurations observed at S_B step edges. The abundances observed for the different configurations are also indicated.

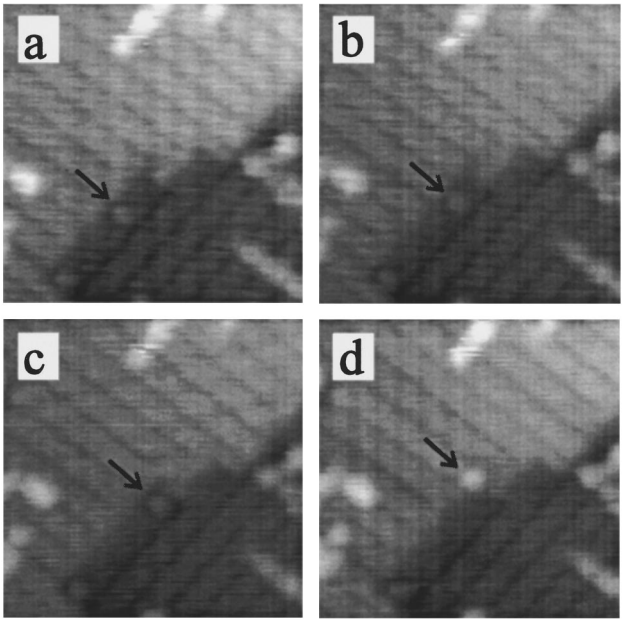

FIG. 3. Subsequent empty-state STM images showing diffusion of an adatom along a rebonded S_B step edge (a–c). In (d) the adatom climbs to the upper terrace at a kink site. Tunneling conditions 0.4 nA, −1.6 V.

formed [see configuration 4 in Figs. 1(g) and 1(h)]. For an epitaxial dimer the dimer bond should have been perpendicular to those of the lower terrace. Configuration 4 can be formed from a second adatom on the lower terrace dimerizing with the adatom of configuration 1*a*. It should be noted that configuration 2, which also requires the arrival of two adatoms, has a very low abundance with respect to configuration 4. Configuration 5 in Figs. 1(e) and 1(f) shows an epitaxial dimer which is separated from the upper terrace dimer row by a vacancy. Their abundance amounts to about 1% of the dimer row ends. Single adatoms can also be attached to the configurations 4 and 5. In case of configuration 4 this yields the formation of a three-atom cluster,[14] right at the step edge, as has been observed a few times. Attachment of an adatom at configuration 5 yields the configuration 6 shown in Figs. 1(i) and 1(j): Apart from the vacancy it is similar to configuration 1*a*.

A better understanding of the different bonding topologies can be obtained by using simple tight binding arguments. The unreconstructed Si(001) surface contains two dangling bonds per surface atom. Upon reconstruction dimers are formed and the dangling bonds form a strong σ-like bonding state and a much weaker π-like bonding state. Configuration 0 is stabler than configuration 2, because adding a dimer to the former requires the breaking of two strong σ bonds, whereas adding a dimer to the latter only requires the breaking of two weak π bonds. In configuration 0 the π bonds of the lower terrace dimer at the step edge are broken. This yields semifilled dangling bonds which are visible in both the filled and the empty-state image [see Figs. 1(a) and 1(b]. These dangling bonds act as reactive sites for adatom adsorption.[19] Furthermore, binding at the reactive sites is stabler than binding at an ordinary substrate dimer row, where the π bonds are still intact. This explains why at room temperature single adatoms can be seen bound to a step edge.

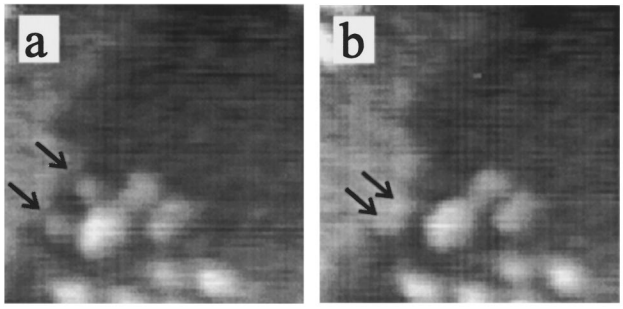

FIG. 4. The formation of a dimer from two adatoms bound at a rebonded S_B step edge in between two subsequent empty-state STM images. Tunneling conditions: 0.4 nA, −1.7 V.

Changes in step edge configurations observed with STM yield information about the dynamic processes involved in step-flow growth. Figures 3(a)–3(c) show the hopping of an adatom along the step edge, subsequently sampling the configurations 1*a*, 1*b*, and 1*a*. As Fig. 1(d) shows, the adatom finally climbs to the upper terrace at the kink site. Whether the stable binding of the adatom at that site results from the kink configuration or from the presence of a second adatom, could not be concluded unambiguously. Two adatoms diffusing along a rebonded S_B step edge can form a dimer together, as shown in Fig. 4. This demonstrates a pathway for the formation of configuration 2. We have also observed the reverse process of breaking such a dimer at a nonrebonded S_B step edge.

The binding sites for adatoms at rebonded S_B step edges are stable as most of these adatoms do not move during the capturing of subsequent STM images at room temperature. This observation of an increased barrier for diffusion onto the terrace is in accordance with *ab initio* calculations,[12,13] which predict the energy of the binding site in configuration 1*a* to be at least 0.5 eV lower than the global minimum for an adatom on the terrace. In these calculations a low activation energy was found for the diffusion over the top of the lower terrace dimer row next to the step edge. In our observations we see that an adatom diffusing along the step edge samples all the intermediate binding sites (see Fig. 3). Thus, the effective diffusion rate along the rebonded S_B step edge is strongly reduced by the frequent sidesteps of the diffusing adatom to the more stable sites in the configurations 1*a* and 1*b*.

If growth is performed at elevated temperatures, ad dimers also become mobile and can stick to step edges directly. In that case the step edge subsequently assumes the configurations 0 and 2 [see Figs. 1(a)–1(d) and 2]. In general, adatoms have a much higher mobility and, therefore, will arrive at the step edges more easily than ad dimers. Whether the sticking of complete dimers is relevant during step-flow growth depends on the sticking coefficient for single adatoms at the various step edge configurations.

The observation of configuration 5 indicates the existence of another important dynamic process at the step edge: the creation of vacancies. Rotation of the nonepitaxial dimer in configuration 4 may account for the formation of configuration. However, configuration 4 is generally formed by adding two adatoms to an otherwise straight step edge, as can be seen in Figs. 1(g) and 1(h), while in most cases configuration

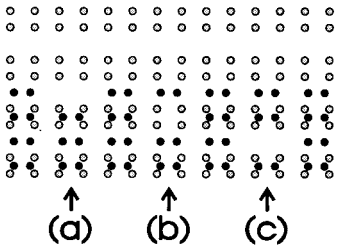

FIG. 5. Schematic representation of the formation of a single dimer vacancy [(b): configuration 5] at a nonrebonded S_B step edge [(a): configuration 2]. The single dimer vacancy can diffuse along the dimer rows of the terrace (c).

5 consists of a vacancy just behind a straight step edge as depicted schematically in Fig. 5(b). This points towards another mechanism for the formation of configuration 5. As shown in Figs. 5(a) and 5(b) the outer dimer in configuration 2 may jump into the trough and leave a single dimer vacancy behind. This transition is reasonable in view of the high energy of configuration 2. The vacancy created just behind the step may now diffuse across the terrace [see Fig. 4(c)] with the typical activation energy required for vacancy diffusion.[17] The above process for the creation of single dimer vacancies is likely to have a lower activation energy than their creation somewhere on the terrace. Thus, the density of vacancies on the terrace should be intimately related to step edge processes.

We conclude that STM studies of growth at step edges should involve empty-state images, as only these images show the undimerized atoms. A number of different step edge configurations are described. These configurations represent the different stages of the growth at S_B step edges using single adatoms. The existence of competitive processes yielding nonepitaxial structures at the step edges is also demonstrated. Furthermore, the processes of adatom diffusion along the step edges and dimerization of two such adatoms are visualized directly. Finally, we propose a low activation energy pathway for the creation of single dimer vacancies at the step edges.

[1] D. J. Chadi, Phys. Rev. Lett. **59**, 1691 (1987).
[2] A. J. Hoeven, J. M. Lenssinck, D. Dijkkamp, E. J. van Loenen, and J. Dieleman, Phys. Rev. Lett. **63**, 1830 (1989).
[3] R. J. Hamers, R. M. Tromp, and J. E. Demuth, Phys. Rev. B **34**, 5343 (1986).
[4] H. J. W. Zandvliet, H. B. Elswijk, and E. J. van Loenen, Surf. Sci. **272**, 264 (1992).
[5] N. Kitamura, B. S. Swartzentruber, M. G. Lagally, and M. B. Webb, Phys. Rev. B **48**, 5704 (1993).
[6] B. S. Swartzentruber and M. Schacht, Surf. Sci. **322**, 83 (1995).
[7] C. Pearson, B. Borovsky, M. Krueger, R. Curtis, and E. Ganz, Phys. Rev. Lett. **74**, 2710 (1995).
[8] C. Pearson, M. Krueger, R. Curtis, B. Borovsky, X. Shi, and E. Ganz, J. Vac. Sci. Technol. A **13**, 1506 (1995).
[9] R. A. Wolkow, Phys. Rev. Lett. **74**, 4448 (1995).
[10] P. J. Bedrossian, Phys. Rev. Lett. **74**, 3648 (1995).
[11] Z. Zhang, Y.-T. Lu, and Horiz Metiu, Surf. Sci. Lett. **255**, L543 (1991).
[12] Q. M. Zhang, C. Roland, P. Boguslawski, and J. Bernholc, Phys. Rev. Lett. **75**, 101 (1995).
[13] J. Wang, D. A. Drabold, and A. Rockett, Surf. Sci. **344**, 251 (1995).
[14] J. van Wingerden, A. van Dam, M. J. Haye, P. M. L. O. Scholte, and F. Tuinstra, Phys. Rev. B **55**, 4723 (1997).
[15] K. Besocke, Surf. Sci. **181**, 145 (1987).
[16] A. van Dam, J. van Wingerden, M. J. Haye, P. M. L. O. Scholte, and F. Tuinstra, Phys. Rev. B **54**, 1557 (1996).
[17] N. Kitamura, M. G. Lagally, and M. B. Webb, Phys. Rev. Lett. **71**, 2082 (1993).
[18] G. Brocks and P. J. Kelly, Phys. Rev. Lett. **76**, 2362 (1996).
[19] G. Brocks, P. J. Kelly, and R. Car, Phys. Rev. Lett. **66**, 1729 (1991).